Light-Induced Charged and Trap States in Colloidal Nanocrystals Detected by Variable Pulse Rate Photoluminescence Spectroscopy

Michele Saba,[†,*] Mauro Aresti,[†] Francesco Quochi,[†] Marco Marceddu,[†] Maria Antonietta Loi,[‡] Jing Huang,[§] Dmitri V. Talapin,[§] Andrea Mura,[†] and Giovanni Bongiovanni[†,*]

[†]Dipartimento di Fisica, Università di Cagliari, I-09042 Monserrato, Italy, [‡]Zernike Institute for Advanced Materials, University of Groningen, Groningen 9747 AG, The Netherlands, and [§]Department of Chemistry, The University of Chicago, Chicago, Illinois 60637, United States

ABSTRACT Intensity instabilities are a common trademark of the photoluminescence of nanoemitters. This general behavior is commonly attributed to random fluctuations of free charges and activation of charge traps reducing the emission yield intermittently. However, the actual physical origin of this phenomenon is actively debated. Here we devise an experiment, variable pulse rate photoluminescence, to control the accumulation of charges and the activation of charge traps. The dynamics of these states is studied, with pulse repetition frequencies from the single-pulse to the megahertz regime, by monitoring photoluminescence spectrograms with picosecond temporal resolution. We find that both photocharging and charge trapping contribute to photoluminescence quenching, and both processes can be reversibly induced by light. Our spectroscopic technique demonstrates that charge accumulation and trap formation are strongly sensitive to the environment, showing different dynamics when nanocrystals are dispersed in solution or deposited as a film.

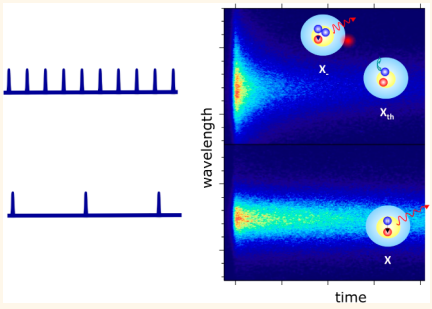

KEYWORDS: ultrafast spectroscopy · colloidal nanocrystals · photoluminescence · traps

Colloidal semiconductor nanocrystals hold great promise for a wide variety of photonic applications owing to their tunable optical gaps and their facile processing. Nanocrystals have been demonstrated as light sources in applications ranging from bioimaging to super-resolution optical microscopy in life sciences, from single-photon guns to nanophotonic circuits in information and communications technology, and from light-emitting diodes to lasers in optoelectronics. The effective, and often the optimal, operating condition for many of these photonic applications is the single-excitation regime, with less than one excited electron–hole pair per nanocrystal at any given time but a large repetition rate of emission events, possibly approaching the steady-state limit.[1−4] The resulting challenge is to design nanostructures capable of emitting light with high efficiency and stability in these working conditions.

Considerable hindrance is therefore caused by the fact that, under steady-state operation, the intensity of the light emitted from a nanosized source tends to be unstable, randomly blinking over time. This ubiquitous phenomenon has been observed for many years in molecular systems and nanostructures.[5−13] More stable emission has been recently achieved by a proper design of the overcoating inorganic shells in colloidal quantum dots.[14−19] Yet, the origin of the emission instabilities is still controversial in prototype nanostructured materials, such as colloidal quantum dots, and is currently the subject of ongoing debates. A large part of the existing literature assumes that fluorescence intermittency is caused by charging and discharging of nanocrystals,[15−18,20−30] based on the well-established experimental evidence that charged quantum dots are weak emitters owing to fast nonradiative Auger recombination of excitons.[1−4,31] Recent experimental results and new theoretical models indicate, however, that fluorescence intermittency may have a different origin, triggered by random activation of

* Address correspondence to saba@unica.it, giovanni.bongiovanni@dsf.unica.it.

Received for review August 27, 2012 and accepted November 29, 2012.

Published online 10.1021/nn305031k

nonradiative exciton traps at the nanocrystal surface.[5−12,32−44] Whether or not these emission instabilities can be indirectly induced, or influenced by light, as recently suggested, is still an open question.[14−19,29,37,45]

Experiments aimed at identifying the fundamental mechanisms of photoluminescence quenching so far have taken advantage of single-molecule optical spectroscopy techniques. Here, we report on a different approach, based on transient nonlinear photoluminescence spectroscopy applied to an ensemble of nanocrystal quantum dots. This spectroscopic tool represents a variation on the well-established approach to the dynamics of multiple electron−hole pairs in the regime of high fluence excitation.[15−18,20−30,46] We tailored the technique to investigate basic emission quenching processes appearing at injection levels below one electron−hole pair per nanocrystal per excitation pulse. The key idea is to control the repetition rate and energy of the excitation laser pulses to induce the pile-up of long-lived, nonradiative states surviving in quantum dots from one pulse to the next one. Light-induced quenching processes are then monitored through detection of nonlinear transient photoluminescence. While the technique accesses a long-lived state, a major advantage of variable repetition rate photoluminescence is to retain the full picosecond temporal resolution of ultrafast photoluminescence necessary to detect directly quenching phenomena.

Variable pulse rate photoluminescence spectroscopy is applied here to CdSe/CdS core/shell nanocrystals, in order to control and investigate dark and weakly emitting states in a model system, known for high luminescence quantum yield and reduced blinking. We are able to distinguish between contributions to the emission dynamics due to excitons created in nanocrystals with charged cores from those with active charge traps. We identify the spectroscopic features of both negative and positive trions, their characteristic relaxation times, and the photoinduced trapping kinetics of neutral excitons. We observe that accumulation of charges and the population of trap centers saturate for increasing light intensity in nanocrystal films. From the saturation dynamics, we deduce a lifetime of negatively charged cores on the order of tens of microseconds in nanocrystal films. On the other hand, we have found no specific time scale associated with trap states in nanocrystals in a liquid dispersion, a behavior we tentatively ascribe to nanocrystal interactions with solvent and to the dynamic attachment of ligands. We also find that nanocrystal photoionization occurs through Auger processes and show that multiexciton states have a low photoionization yield, around 10^{-3}−10^{-4}.

RESULTS AND DISCUSSION

In the top panel in Figure 1, possible states contributing to a transient photoluminescence signal at energies resonant with the band edge are sketched. The fundamental optical excitations, band edge excitons (X), are created in neutral nanocrystals by the absorption of a laser photon and subsequent relaxation of electron and hole to the band edge. Trions or charged excitons (X_+ and X_-) are created by optical absorption in a charged nanocrystal, that is, a nanocrystal left over by previous laser pulses in a long-lived, charge-separated state, with a positive or negative charge inside the core, while the opposite charge is trapped in a state on the surface or outside the nanocrystal. Trions contribute to band edge photoluminescence, but with a faster radiative emission rate and therefore a larger prompt intensity with respect to neutral excitons, owing to the fact that statistics allow twice as many recombination paths for trions than for excitons.[47] Trapping of electrons or holes after the exciton has relaxed (trapping of thermal excitons, X_{th}) represents a nonradiative recombination channel reducing the lifetime of excitons and therefore the photoluminescence decay time. On the other hand, trapping of hot photoexcited carriers before they relax (trapping of hot excitons, X_h) occurs in a picosecond time scale and therefore reduces the photoluminescence intensity without affecting its decay time as measured with our streak camera. Finally, absorption of two photons from the same laser pulse may create a biexciton (bX) in the nanocrystal; such a state has a 4 times larger radiative recombination rate with respect to excitons and therefore produces a larger transient photoluminescence signal but is also subject to fast nonradiative Auger recombination and therefore a lifetime typically much shorter than the exciton one (in the Supporting Information, the effects on photoluminescence decays caused by each of the above-mentioned states are sketched).[31] Multiexciton states with multiplicity larger than two are not included in this analysis because they can be identified by their emission at photon energies substantially larger than the band gap and they decay into band edge states in a very short transient, on the order of 10 ps.

The bottom right panel in Figure 1 illustrates the potential of nonlinear photoluminescence spectroscopy to investigate emission quenching and to distinguish light emission from neutral, positively, and negatively charged quantum dots. The two different spectrograms in the figure were taken on a nanocrystal film excited with the same laser pulse energy (corresponding to an average number of excitations per nanocrystal $N = 0.16$), but with two very different pulse repetition rates (4 MHz and 800 Hz): while low repetition pulse train generated only exciton states, high repetition pulses caused pile-up of long-lived charge-separated states, resulting in faster decaying emission from trions and a wider photoluminescence spectrum. In the following, we will fully explore the potential of variable pulse rate photoluminescence to controllably induce charged states and quantitatively determine their properties.

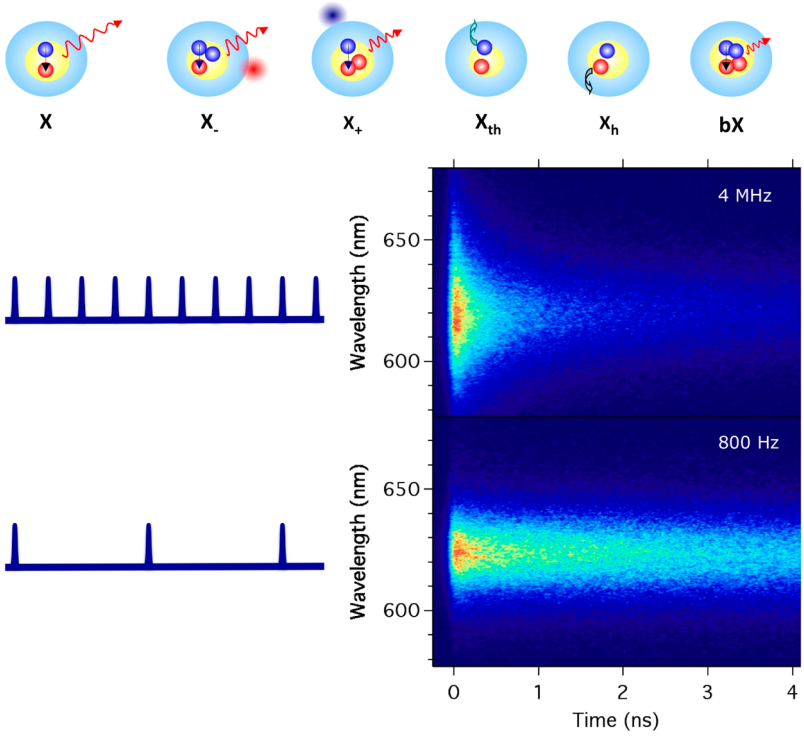

Figure 1. Top panel: sketch of the states contributing to the dynamics of band edge photoluminescence, in order excitons, negative and positive trions, thermal traps, hot traps and biexcitons (see the text for a discussion of their respective effects on the measured emission signal). Bottom left panel: sketch of the laser pulse train (repetition frequency and pulse duration are not to scale with respect to each other) before and after pulse picking. Bottom right panel: streak camera photoluminescence spectrograms in nanocrystal films taken with two different pulse repetition rates, but with the same energy per pulse, corresponding to $N = 0.16$.

Figure 2a–c shows the time-resolved photoluminescence traces from a nanocrystal toluene dispersion as a function of the laser repetition rate (ν), operating at fixed pulse energies; that is, in each panel, the number of photogenerated electron–hole pairs per dot per excitation pulse is kept constant ($N = 0.0028$, 0.09, 0.28, respectively); ν ranges from 400 Hz to 4 MHz. At very low excitation fluences ($N < 0.003$, Figure 2a), the decay time of the emission signal is independent of pulse fluence and repetition rate, indicating that light emission comes from the radiative decay of single excitons, while the population of multiexcitons, trions, and photoactivated trap states is negligible. For higher laser pulse fluence, namely, generating $N = 0.09$ excitons per nanocrystal (Figure 2b), a weak component with a fast decay is observed. However, repetition frequency does not affect transient emission, a clear indication that the short-lived signal is due to nanocrystals doubly excited by a single laser pulse (*i.e.*, to biexcitons), while there is no accumulation of charged states from pulse to pulse. At all excitation fluences and intensities, the photoluminescence decay rate of the single-exciton emission is recovered at long delays. This excitonic contribution for each transient photoluminescence is marked by a red trace with amplitude A_x and corresponds to the emission signal recorded in the single-exciton regime ($N = 0.0028$), rescaled to match the overall dot emission at the specific excitation fluence for time delays longer than 15 ns. The difference between the emission signal and the excitonic contribution, highlighted in cyan, provides a direct visualization of the short-lived nonlinear photoluminescence [NLPL(t)]. Figure 2c shows that frequency-dependent quenching mechanisms manifest only at the highest fluences ($N = 0.28$) as a decrease of the emission signal for intermediate pulse repetition frequencies, $\nu = 800$ kHz. The reduction of the prompt photoluminescence, A_0, suggests that the laser pulse train induces the activation of trapping sites, which capture hot charged carriers before they can radiatively recombine. However, trap centers are not activated permanently, but are reversibly switched on and off in relation with the effective pulse fluence and repetition frequency.

Figure 2d–f highlights how charged states and traps depend on the environment surrounding nanocrystals. The figure panels report the photoluminescence emission decays obtained from a drop-cast nanocrystal thin film; as for the liquid sample, the number of absorbed electron–hole pairs per dot per excitation pulse was kept constant for each series. Figure 2d,e shows that the transient photoluminescence in the single-exciton regime, $N = 0.0075–0.016$, is frequency-independent. Only for excitation levels of $N = 0.16$, short-lived components are visible (Figure 2f). In such conditions,

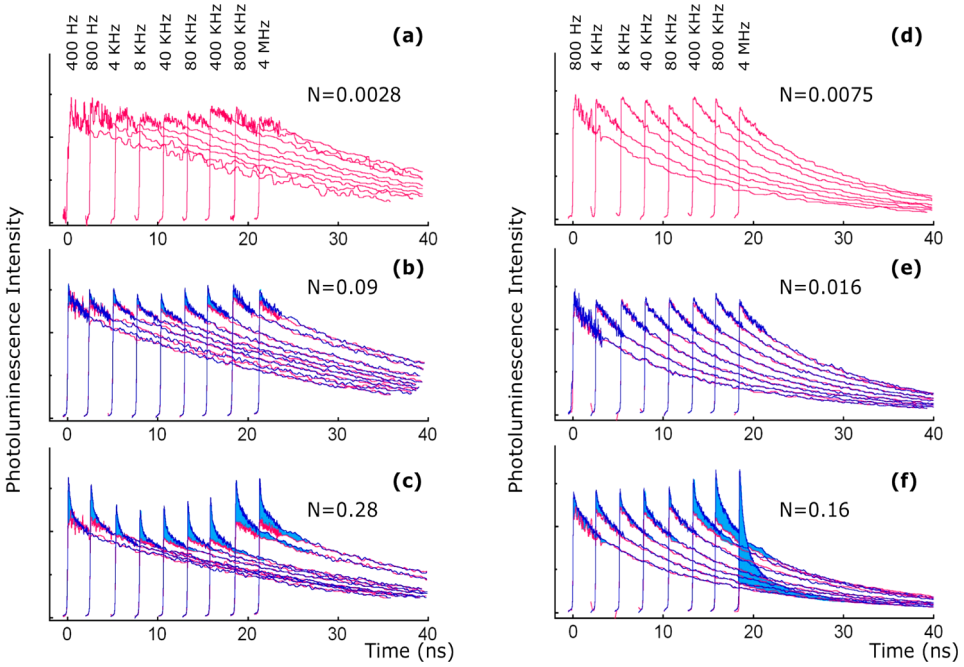

Figure 2. Photoluminescence decays (blue lines) corresponding to nine excitation pulse rates for three pulse fluences. Emission decays from nanocrystal solutions are reported in panels (a−c), from nanocrystal films in panels (d−f). To better visualize all transient emission traces, decays are shifted to the right for increasing repetition frequency. Laser pulse fluence rises from top to bottom. Blue regions highlight the nonlinear emission signal, while red lines represent the excitonic contribution. At a fixed pulse fluence, this contribution was estimated by taking the emission signal recorded at very low excitation (solution: $N = 2.8 \times 10^{-3}$; film: $N = 7.5 \times 10^{-3}$), rescaled to match the higher excitation photoluminescence transient at time delays longer than 15 ns.

the phenomenology appears different with respect to the liquid sample. At low frequencies, fast contributions show an amplitude and lifetime consistent with the presence of a small biexciton population. Quenching mechanisms become very effective at high pulse repetition rate, with a frequency threshold at 80 kHz. At the largest frequency, 4 MHz, the long-lived exciton contribution decreases down to 20% of the low-frequency signal, while the enhancement of the prompt emission signal is symptomatic of the formation of a charged exciton population.

The number of available pulse repetition frequencies above the threshold for emission quenching is limited by experimental constraints. To access a more detailed analysis of the quenching mechanisms, we therefore study the nonlinear response as a function of a complementary parameter controlling the accumulation of long-lived nanocrystal states, the pulse fluence, which we can finely tune. In analyzing results, one has however to account for the nonconstant contribution of multiexciton states to photoluminescence. Figure 3 shows the prompt photoluminescence intensity and the contribution of single excitons extrapolated at time zero (A_0 and A_x, respectively) as a function of N for $\nu = 4$ MHz. Transient emission traces used to extract the amplitudes are reported in the Supporting Information. At low pulse fluences, the photoluminescence intensity grows linearly. At a threshold of about 0.05 exciton per nanocrystal, the long-lived emission starts saturating, while the

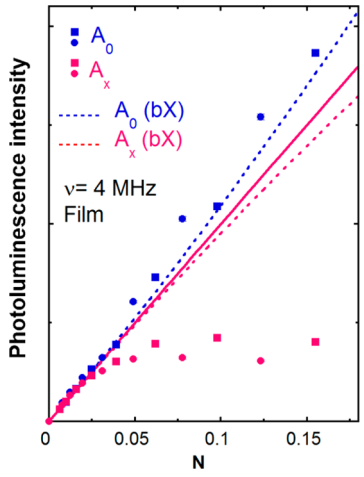

Figure 3. Prompt photoluminescence signal (A_0, blue circles) and contribution to the experimental emission intensity originating from long-lived excitons (A_x, red circles) as a function of the average number of injected electron−hole pairs per dot (N). The tick red line represents a linear fit to $A_0(N)$ in the low excitation regime ($N < 0.025$). The two dashed lines represent the amplitudes expected for A_0 and A_x accounting only for biexciton effects, in the absence of trions and traps. Transient emissions were recorded in two different pulse energy scans. The second one was acquired 2 h later and is marked by squares. The photoluminescence time traces from which intensities are extracted can be found in the Supporting Information.

prompt response shows a slightly superlinear behavior. Remarkably, such saturation occurs for an average excitation N at least an order of magnitude lower than

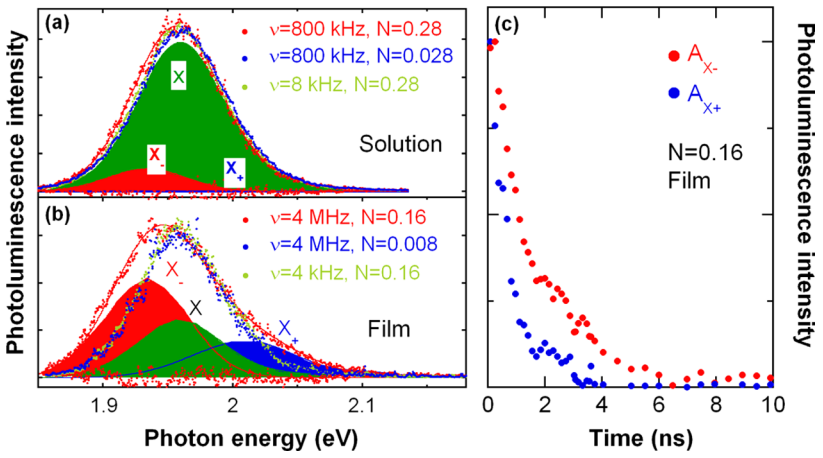

Figure 4. Photoluminescence spectrum (dots) recorded in a time window (Δt = 0.1 ns) centered at t = 0.6 ns, in a nanocrystal (a) solution and (b) film. Red continuous lines are fits to emission spectra at the highest pulse fluence and repetition rates (film: ν = 4 MHz, N = 0.16; solution ν = 800 kHz, N = 0.28). Residuals from fits are also shown. X_+, X_-, and X represent emissions, as obtained from the fit analysis, due to positive and negative trions and excitons, respectively. (c) Decays of the trion amplitudes assessed from the fits as a function of time.

the standard saturation associated with state filling and is only observed at high laser pulse repetition rate; for ν = 800 Hz, saturation effects up to N = 0.16 are negligible, as noticeable by a critical inspection of Figure 2f. The two dashed lines represent the amplitudes expected for A_0 and A_x accounting only for biexciton effects, in the absence of trions and traps.

Experimental results in Figure 3 are representative of two different intensity scans, acquired with a 2 h delay between them, and identified respectively by round and square markers; for increasing number of electron–hole pairs injected per nanocrystal, experimental points belong alternatively to the first and second run. The two data sets show the degree of reversibility of photoinduced changes in the transient photoluminescence signal. In the delayed experiment, a higher long-lived excitonic emission is accompanied by a lower enhancement of the prompt signal. This correlation indicates that a prolonged illumination mainly reduces the efficiency of light-induced nanocrystal charging.[48,49] Since the amplitudes of photoluminescence components related to traps show very little hysteresis effects when the laser fluence is scanned across the threshold for trap activation, we define trap activation as a reversible effect, apparently not entailing permanent modifications of nanocrystals or their surface ligands.

Figure 3 demonstrates that quenching mechanisms for N = 0.15 are so efficient that about two over three excitons decay nonradiatively. If quenching were due to nanocrystal charging, two-thirds of the photoexcitations should be charged excitons, with faster radiative time than excitons, resulting in a large enhancement (~5/3) of the prompt emission signal with respect to the case in which only neutral excitons were created (red line in Figure 3). The weak enhancement of the prompt signal A_0 and the large reduction in the single-exciton contribution A_x therefore indicate that light-induced trap states also contribute to photoluminescence quenching. Experiments performed in different films showed similar results, even though the absolute and relative weight of charged states and trap centers to photoluminescence quenching are found to vary from film to film and with film aging.

Spectral analysis of the photoluminescence emission provided additional direct evidence of the contribution of trions to band edge photoluminescence. Figure 4 shows transient photoluminescence spectra extracted from streak camera spectrograms in a time gate of 0.1 ns close to 0.6 ns delay time, for both toluene dispersion (a) and drop-cast film (b) samples. In solution, spectra at high and low excitation level are very similar, and only a slight red shift is observed at high excitation and high repetition rate. In the film instead, at high repetition rate and excitation level of 0.16 electron–hole pair injected per dot per pulse, the transient spectrum reveals a red-shifted emission with respect to the low-excitation spectrum; a weaker, blue-shifted component also appears. We attribute these two components respectively to negatively[50,51] and positively[52,53] charged nanocrystals. Concerning biexcitons, their emission spectrum, measured with the setup for single-shot measurements described in the Supporting Information, could not be distinguished from the excitonic one; therefore, spectral analysis does not provide information on biexcitons. We analyze spectra by deconvolving them as the sum of the low-fluence exciton emission line shape and two Gaussians for the positive and negative trions, respectively. A global fit of all transient spectra of nanocrystals in dispersion and in film gave trion binding energies of -25 ± 5 and $+50 \pm 20$ meV, respectively, for negatively and positively charged excitons. Fitting the spectrum as a function of time and measuring the weight in the spectrum of the two lateral Gaussian curves, we are therefore able

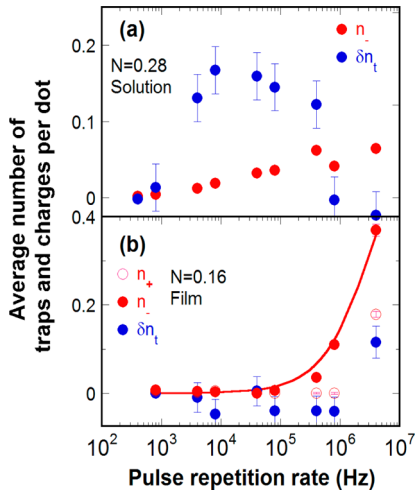

Figure 5. Photoinduced traps and charges as a function of the pulse repetition frequency in nanocrystal solutions (a) and films (b). Fraction of nanocrystals with an additional negative (n_-) and positive (n_+) charge, and with a light-activated charge trap $\delta n_t(\nu) = n_t(\nu) - n_t(\nu_0)$. $\delta n_t(\nu)$ accounts for the photoinduced trap population with respect to the data taken at the reference frequency ν_0 fixed to 400 and 800 Hz in solution and films, respectively. Red line in panel (b) is a curve for the negative charge population calculated according to eq 1, as explained in the text.

to track trion dynamics. The result of the analysis is shown in Figure 4c. At delays longer than the biexciton lifetime (τ_{bX}), the decay time of the photoluminescence signal can be safely ascribed to radiative recombination of neutral and charged excitons alone. The transient traces for $t > \tau_{bX}$ are then used to assess the lifetime of negative and positive trions. The accurate determination of τ_{bX} and the procedures used to determine the photoluminescence lifetimes for $t > \tau_{bX}$ are described in the Supporting Information; we find $\tau_{bX} = 0.40 \pm 0.03$ ns, $\tau_{X-} = 2.3 \pm 0.2$ ns, and $\tau_{X+} = 1.1 \pm 0.2$ ns. The experimental values of the nonradiative decay times of trions and neutral biexciton (τ_{bX}) satisfy the relation $1/\tau_{bX} \sim 2/\tau_{X-} + 2/\tau_{X+}$, as one could expect from statistics arguments and in excellent agreement with the pseudopotential theory of Auger lifetimes in colloidal quantum dots.[54]

Thanks to spectral deconvolution of transient photoluminescence spectra, we determine the amplitude of the trion photoluminescence. Trion states are created with low fluence excitation, generating on average much less than one electron−hole pair per nanocrystal, only assuming that a fraction of nanocrystals are left charged by previous laser pulse excitation. We label n_+ and n_- the fraction of positively and negatively charged nanocrystals, whose excitation leads to X_+ and X_-, respectively, in each nanocrystal. The fraction of negative and positive trions with respect to exciton population in turn is used to infer the steady-state population of charged nanocrystal states n_+ and n_-, the precursor states that lead to trions upon optical excitation. Analogously, we define n_h and n_{th} as the average number of hot charge (X_h) and thermal charge (X_{th}) traps per nanocrystal. Details on the procedures used to assess charge (n_- and n_+) and trap (n_h and n_{th}) populations are reported in Supporting Information. Figure 5 shows the steady-state population of the charged nanocrystal state as a function of excitation conditions, resulting from the analysis of both film and dispersion. By measuring the amplitude A_x of the single-exciton component surviving for a long time after excitation, we also measure the yield for generation of single excitons and therefore extract the number of light-activated traps. We call the total population of trap states $n_t = n_h + n_{th}$ the sum of hot charge (n_h) and thermal charge (n_{th}) traps. In principle, n_t could include a background population of static traps, which are independent of pulse fluence and repetition frequency. Figure 5 therefore reports the quantity $\delta n_t(\nu) = n_t(\nu) - n_t(\nu_0)$, which accounts for the photoinduced trap population with respect to the data taken at the reference frequency ν_0 fixed to 400 Hz. Finally, from the experimental values of A_x and A_0, we evaluate the photoinduced population of hot charge traps, $\delta n_h(\nu) = n_h(\nu) - n_h(\nu_0)$. We find that $\delta n_h \sim \delta n_t$, within the experimental uncertainty.

In the liquid dispersion (Figure 5a), we observe only emission from negatively charged excitons, whose contribution grows gently as a function of laser repetition frequency, ν, following a logarithmic frequency dependence, with no evident saturation threshold for charge accumulation. In other words, we find no specific time scale associated with the creation of charged states in a liquid environment. Light-activated traps are found to contribute only in a range between 4 and 800 kHz, with values around 0.15 traps per dot. On the other hand, in the film (Figure 5b), the number of charged nanocrystals developing trions instead of excitons is negligible until laser repetition frequency reaches 800 kHz; at such frequency, the contribution of charged states kicks in and grows rapidly as a function of repetition frequency, with more than 35% of nanocrystals ending up negatively charged for $\nu = 4$ MHz. Positive trions are only observed at the highest repetition frequency, where the fraction of quantum dots with a photoinduced extra hole is ~20%. Consequently, more than half of the nanocrystals are charged at this repetition frequency. Concerning traps, we find a sizable trap population, $\delta n_t = 0.1$, only at $\nu = 4$ MHz.

Figure 6 reports the analysis of photoluminescence data as a function of laser fluence, at the fixed frequency of 4 MHz. The average number of traps and charges per dot has been calculated according to the protocol for data analysis used for nanocrystal solutions. At the highest energy per pulse, Figure 6 shows that most of quantum dots are weak emitters (gray states), due to a large photoinduced population of active traps ($n_{th} > n_h$) and the accumulation of a significant charge in the core of nanocrystals.

In a photocharging process, one electron (hole) is ejected outside the nanocrystals or trapped at the

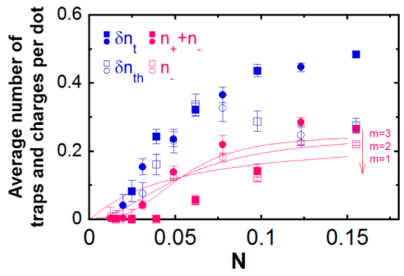

Figure 6. Photoinduced traps and charges as a function of injected electron−hole pairs per dot in nanocrystal films. Fraction of nanocrystals with an extra charge in the core ($n_+ + n_-$), an additional negative charge (n_-), light-activated charge traps (δn_t), and light-activated traps intercepting thermal charges (δn_{th}). Red lines are representative saturation curves for the charge population assuming a characteristic recombination time τ_-. Parameters are chosen to best reproduce the population of negative charges in non-photo-treated films (first scan in Figure 3); m is the power law index (see main text for definitions). Error bars correspond to one standard deviation.

external surface, leaving the core with an unbalanced charge. Such process can start after photoexcitation of a single exciton because of trapping of one of the two charges composing the exciton, or following Auger recombination of a multiexciton state, when one exciton disappears and its energy is conferred to a single charge. In the simplest scenario, called a relaxation time model, split charges recombine with a characteristic lifetime $\tau_{-(+)}$. Quasi-steady-state population of trap states can be assumed when $\nu\tau_{-(+)} \gg 1$, meaning that n_+ and n_- at the arrival of the laser pulse are constant from one pulse to the next. In such condition, the charge population reads

$$n_{-,+} = \frac{N^m \nu \alpha \tau_{-,+}}{N^m \nu \alpha \tau_{-,+} + 1} n_{sat\,-,+} \qquad (1)$$

where α is the probability that the excited state relaxes through nanocrystal ionization, while m is the order of the multiexciton state (mX) at the origin of photocharging (N is the average number of excitons per dot per pulse). At very low excitation intensities, the population scales as $N^m \nu \alpha \tau_{-,+}$. Charge saturation can be induced both by varying pulse repetition frequency ν but fixed N or by varying the pulse fluence, and therefore N, but keeping the repetition frequency ν constant. In the former case, $n_{-,+}$ grows linearly with the pulse repetition frequency ν, as long as $N^m \nu \alpha \tau_{-,+} \ll 1$, and eventually saturates at the value $n_{sat,-,+}$ at high excitation frequencies, when $N^m \nu \alpha \tau_{-,+} \gg 1$. This same saturation value can be obtained raising the excitation fluence.

The sharp rise of n_- in nanocrystal films is well accounted for by eq 1 (Figure 5b). In experiments with fixed laser repetition frequency, but varying pulse fluence, one can expect to infer the origin of charged states from the dependence of $n_{-,+}$ on the mean excitation level, N: in the case of charge splitting in single-exciton states, $m = 1$ and $n_{-,+}$ grows linearly with the mean excitation power, as $N\nu$; if, on the other hand, charge ejection is triggered by Auger processes, $n_{-,+}$ should scale at least quadratically, as $N^m \nu$ (with $m \geq 2$). Figure 6 shows that the simple relaxation time model describes satisfactorily the saturation behavior observed experimentally, demonstrating that generation of negative charges in nanocrystal films is triggered by Auger recombination ($m \sim 2$). The saturation pulse fluence, $N_{sat,-}$, defined as the number of injected electron−hole pairs at which $n_- = n_{sat,-}/2$ ($N^2_{sat,-} \nu \alpha \tau = 1$) can be extracted from the saturation value in Figure 6 and turns out to be 0.05. The value $\alpha \times 10^{-4}$ is determined independently in single-pulse experiments, that is, in the absence of charge accumulation between pulses, by fitting the amplitude of the trion emission as a function of the pulse fluence (see Supporting Information for a detailed description of the procedure). The knowledge of $N_{sat,-}$ and α leads to the determination of the characteristic relaxation time for negative charges, $\tau_- = 6 \times 10^{-2}$ s. The time scale of τ_- is in excellent agreement with estimates obtained in single-nanocrystal experiments.[21,34] In films previously exposed to irradiation, we observe a similar behavior except that the pulse fluence necessary to achieve charge saturation increases owing to photobrightening effects.

In nanocrystal toluene dispersions, contrary to the film samples, photoluminescence experiments show a slow increase of the fraction of negatively charged nanocrystals as a function of ν, with no evidence of saturation (Figure 5a). The stark contrast between charge accumulation behavior in nanocrystal solutions and films points to the key role played by the environment. In solutions, the dependence of n_- on the excitation intensity $N\nu$ strongly deviates from the behavior foreseen by invoking a recombination time $\tau_{-,+}$, as explicitly assumed in eq 1. These findings suggest that the dynamics of the ejected charges could be strongly influenced by stochastic interactions with solvating molecules, resulting in a kinetics that is not characterized by a specific time scale. The importance of interaction with the surrounding medium may stem from the fact that ligands are not covalently anchored to the surface; their surface coverage should instead be seen as the result of the dynamical equilibrium between adsorption and desorption processes.[33,55]

One possible explanation for the activation of trap states is changes in the local configuration of surface atoms and passivating ligands, with jumps between minima of the surface free energy possibly triggered by light. Two possible mechanisms can be envisioned: (i) following optical excitation, the excess photon energy and the annihilation energy of multiexciton states are quickly released to phonons and ligand vibrations, providing in this way the required energy to modify the local surface configuration; (ii) alternatively, or in addition to the

previous mechanism, surface rearrangement could be triggered by interactions with charges created in photoionization processes. The reversibility of the photoinduced activation of trap states suggests that surface atoms and ligands can relax to the original equilibrium configuration in a relatively short time τ_t. Assuming a quasi-steady-state excitation ($\nu\tau_t \gg 1$), the dynamics of trap states should be then described by an equation similar to eq 1.

Connecting the observed trap and charge dynamics with nanocrystal blinking is beyond the scope of this paper. However, a link may be established considering that (i) neutral nanocrystals are bright emitters; (ii) charged excitons are weakly emitting and can be referred to as gray states; (iii) an exciton in the presence of hot charge traps does not fluorescence and therefore behaves as a dark state; finally, (iv) an exciton generated in dots with thermal charge traps decays radiatively with a quantum yield depending on the electron trapping rates. Light emission instabilities at the level of the single nanocrystal are thus expected to result from the transition of the dot from one to another of these states, a change that may be triggered by random interactions with the environment or induced by photon absorption.

CONCLUSION

In conclusion, we have introduced variable pulse rate photoluminescence as an experimental technique to investigate long-lived states in colloidal nanocrystals. We measure lifetimes of single charges in nanocrystals and highlight different trap dynamics in liquid and film environments. We demonstrate that dark and weakly emitting states, originating both from charges or traps, can be reversibly turned on and off by light. In the case of carrier traps, we speculate that light can indirectly induce a reversible local reorganization of capping molecules on the nanocrystal surface. It has to be noted that the mechanisms of light-induced emission quenching revealed in the present experiments show up at injection levels corresponding to the single-exciton regime and repetition rates approaching the continuous wave excitation. The design and engineering of novel colloidal nanocrystals for several photonic applications, such as quantum communications, bioimaging, super-resolution optical microscopy, light detection, and low threshold lasers, will benefit from a deeper knowledge of the class of quenching processes peculiar of quasi-continuous wave excitation regimes and their relationship with surface properties.

METHODS

CdSe/CdS core/shell nanocrystals have been prepared by seeded growth, starting from 3.6 nm CdSe cores, then covered with a CdS shell up to a total size of 8−10 nm.[56,57] The nanocrystals, dispersed in toluene after purification and centrifugation, are capped by a combination of stabilizing agents employed during growth, that is, trioctylphosphine oxide (TOPO), trioctylphosphine (TOP), and hexadecylamine (HDA). The photoluminescence spectrum is centered around 630 nm in wavelength, corresponding to emission from the CdSe core, meaning that even though the optical absorption occurs mostly in the CdS shell, optical excitations relax to the lowest-energy states in the core before emitting. Both toluene dispersions and drop-cast films on microscope slides have been examined. Concentration of nanocrystals in toluene dispersions have been adjusted to keep the optical density of the dispersion inside a 1 mm quartz cuvette within 0.2 at the laser wavelength, ensuring homogeneous laser excitation throughout the cuvette. Considering that the absorption cross section of nanocrystals is 3.8×10^{-15} cm^2 at $\lambda = 390$ nm, the dispersion concentration was 2 μmol/L. Films were prepared by laying a toluene dispersion drop on a microscope glass slide and letting it evaporate under room atmosphere and at room temperature. The coffee stain type aggregation prevents from quoting a meaningful value for nanocrystal concentration on the glass slide.

The laser source for the time-resolved photoluminescence setup is a titanium:sapphire passively mode-locked femtosecond laser (Spectra Physics Tsunami, pumped by a diode-pumped, frequency-doubled Nd:YAG laser, Spectra Physics Millennia), emitting at 780 nm in wavelength, with a 80 MHz repetition rate, 100 fs pulse duration, and 10 nJ energy per pulse. The pulses are then sent to a home-made pulse picker, realized with a single-pass standing-wave acousto-optic crystal, able to extract selected pulses from the laser pulse train at a frequency variable from 400 Hz to 4 MHz, thereby dividing the laser repetition frequency by a factor ranging from 20 to 2×10^5. Laser pulses are then frequency-doubled to 390 nm in wavelength by focusing onto a second-harmonic generation BBO crystal, 1 mm thick. Ultraviolet laser pulses are then directed and focused onto the sample with a quartz lens, down to a 150 μm spot, to excite photoluminescence.

The excitation level of nanocrystals can be expressed as the average number N of excitons injected in each nanocrystal by a laser pulse, which can be in turn calculated by multiplying the photon fluence in each pulse by the absorption cross section of nanocrystals. The number of excitations in individual nanocrystals is distributed randomly according to Poisson statistics, so that both singly and doubly excited nanocrystals can emit under a specific excitation intensity. In order to check the accuracy of our determination of N, we compared the values obtained with the previous method with an alternate determination of the average number of excitations N, directly monitoring the very area of the excited sample from which light is detected: we employed the ratio between singly and doubly excited nanocrystals (the exciton to biexciton ratio); such measurement was performed at in the "single-pulse" regime when contributions from charged states were negligible, as discussed in the Supporting Information. Notably, such determination of N was in agreement with the one calculated by multiplying photon fluence and cross section, confirming the reliability of the estimation for the photon fluence impinging on the sample.

Collection optics focus photoluminescence into a 30 cm focal length spectrometer (Acton 2300i, equipped with a 150g/mm grating); time-resolved detection is performed with a streak camera (Hamamatsu model C5680) operating in single-shot mode, triggered by reference laser pulses. The temporal resolution of the setup is 10 ps with a 1 ns acquisition window, but degrades to 50 ps with a 20 ns temporal range. The laser excitation spot, as focused on the entrance of the spectrometer, is much larger (450 μm) than both the horizontal spectrometer slit aperture (50 μm, determining spectral resolution) and the streak camera photocathode vertical slit (50 μm, determining

temporal resolution). Such aperture therefore acts as a pinhole in the image plane of the sample and ensures that only the very central part of the excited spot on the sample is actually measured.

Conflict of Interest: The authors declare no competing financial interest.

Acknowledgment. Work in Cagliari was partially funded by the Regione Autonoma della Sardegna through PO-FSE Sardegna 2007-2013, L.R.7/2007, "Progetti di ricerca di base orientata", project nos. CRP3-114, CRP-18353, CRP-24978, and "Borse Giovani Ricercatori" (supporting M.M.).

Supporting Information Available: Definition of photoluminescence lifetime, pictorial sketch of the effects of traps and charges on time-resolved photoluminescence traces, description of the experimental setup and detailed results for photoluminescence measurements in the "single-shot" regime, discussion of thermal effects, description of the theoretical model and the equations employed to interpret the data, photoluminescence transients *vs* pulse fluence at $\nu = 4$ MHz. This material is available free of charge *via* the Internet at http://pubs.acs.org.

REFERENCES AND NOTES

1. *Semiconductor and Metal Nanocrystals: Synthesis and Electronic and Optical Properties (Optical Science and Engineering)*, 1st ed.; Klimov, V. I., Ed.; CRC Press: Boca Raton, FL, 2003.
2. Yin, Y.; Alivisatos, A. P. Colloidal Nanocrystal Synthesis and the Organic–Inorganic Interface. *Nature* **2005**, *437*, 664–670.
3. *Semiconductor Nanocrystal Quantum Dots: Synthesis, Assembly, Spectroscopy and Applications*, 1st ed.; Rogach, A., Ed.; Springer: Berlin, 2010.
4. Talapin, D. V.; Lee, J.-S.; Kovalenko, M. V.; Shevchenko, E. V. Prospects of Colloidal Nanocrystals for Electronic and Optoelectronic Applications. *Chem. Rev.* **2010**, *110*, 389–458.
5. Nirmal, M.; Dabbousi, B.; Bawendi, M. G.; Macklin, J.; Trautman, J.; Harris, T.; Brus, L. E. Fluorescence Intermittency in Single Cadmium Selenide Nanocrystals. *Nature* **1996**, *383*, 802–804.
6. Shimizu, K.; Neuhauser, R.; Leatherdale, C. A.; Empedocles, S.; Woo, W.-K.; Bawendi, M. G. Blinking Statistics in Single Semiconductor Nanocrystal Quantum Dots. *Phys. Rev. B* **2001**, *63*, 205316.
7. Peterson, J.; Krauss, T. Fluorescence Spectroscopy of Single Lead Sulfide Quantum Dots. *Nano Lett.* **2006**, *6*, 510–514.
8. Wang, S.; Querner, C.; Fischbein, M. D.; Willis, L.; Novikov, D. S.; Crouch, C. H.; Drndic, M. Blinking Statistics Correlated with Nanoparticle Number. *Nano Lett.* **2008**, *8*, 4020–4026.
9. Spinicelli, P.; Buil, S.; Quelin, X.; Mahler, B.; Dubertret, B.; Hermier, J.-P. Bright and Grey States in CdSe–CdS Nanocrystals Exhibiting Strongly Reduced Blinking. *Phys. Rev. Lett.* **2009**, *102*, 136801.
10. Crouch, C. H.; Sauter, O.; Wu, X.; Purcell, R.; Querner, C.; Drndic, M.; Pelton, M. Facts and Artifacts in the Blinking Statistics of Semiconductor Nanocrystals. *Nano Lett.* **2010**, *10*, 1692–1698.
11. Ye, M.; Searson, P. Blinking in Quantum Dots: The Origin of the Grey State and Power Law Statistics. *Phys. Rev. B* **2011**, 84.
12. Osborne, M. A.; Lee, S. F. Quantum Dot Photoluminescence Activation and Decay: Dark, Bright, and Reversible Populations in ZnS-Capped CdSe Nanocrystals. *ACS Nano* **2011**, *5*, 8295–8304.
13. Riley, E. A.; Hess, C. M.; Reid, P. J. Photoluminescence Intermittency From Single Quantum Dots to Organic Molecules: Emerging Themes. *Int. J. Mol. Sci.* **2012**, *13*, 12487–12518.
14. Brokmann, X.; Giacobino, E.; Dahan, M.; Hermier, J.-P. Highly Efficient Triggered Emission of Single Photons by Colloidal CdSe/ZnS Nanocrystals. *Appl. Phys. Lett.* **2004**, *85*, 712–714.
15. Mahler, B.; Spinicelli, P.; Buil, S.; Quelin, X.; Hermier, J.-P.; Dubertret, B. Towards Non-blinking Colloidal Quantum Dots. *Nat. Mater.* **2008**, *7*, 659–664.
16. Chen, Y.; Vela, J.; Htoon, H.; Casson, J. L.; Werder, D. J.; Bussian, D. A.; Klimov, V. I.; Hollingsworth, J. A. "Giant" Multishell CdSe Nanocrystal Quantum Dots with Suppressed Blinking. *J. Am. Chem. Soc.* **2008**, *130*, 5026–5027.
17. Spinicelli, P.; Mahler, B.; Buil, S.; Quélin, X.; Dubertret, B.; Hermier, J.-P. Non-blinking Semiconductor Colloidal Quantum Dots for Biology, Optoelectronics and Quantum Optics. *ChemPhysChem* **2009**, *10*, 879–882.
18. Wang, X.; Ren, X.; Kahen, K.; Hahn, M.; Rajeswaran, M.; Maccagnano-Zacher, S.; Silcox, J.; Cragg, G. E.; Efros, A. L.; Krauss, T. Non-blinking Semiconductor Nanocrystals. *Nature* **2009**, *459*, 686–689.
19. Qin, W.; Shah, R. A.; Guyot-Sionnest, P. CdSeS/ZnS Alloyed Nanocrystal Lifetime and Blinking Studies Under Electrochemical Control. *ACS Nano* **2012**, *6*, 912–918.
20. Efros, A.; Rosen, M. Random Telegraph Signal in the Photoluminescence Intensity of a Single Quantum Dot. *Phys. Rev. Lett.* **1997**, *78*, 1110–1113.
21. Gómez, D. E.; van Embden, J.; Mulvaney, P.; Fernée, M. J.; Rubinsztein-Dunlop, H. Exciton-Trion Transitions in Single CdSe–CdS Core–Shell Nanocrystals. *ACS Nano* **2009**, *3*, 2281–2287.
22. Zhao, J.; Nair, G.; Fisher, B. R.; Bawendi, M. G. Challenge to the Charging Model of Semiconductor-Nanocrystal Fluorescence Intermittency from Off-State Quantum Yields and Multiexciton Blinking. *Phys. Rev. Lett.* **2010**, *104*, 157403.
23. Rosen, S.; Schwartz, O.; Oron, D. Transient Fluorescence of the Off State in Blinking CdSe/CdS/ZnS Semiconductor Nanocrystals Is Not Governed by Auger Recombination. *Phys. Rev. Lett.* **2010**, *104*, 157404.
24. Xu, Z.; Cotlet, M. Photoluminenscence Blinking Dynamics of Colloidal Quantum Dots in the Presence of Controlled External Electron Traps. *Small* **2011**, *8*, 253–258.
25. Muller, J.; Lupton, J. M.; Rogach, A. L.; Feldmann, J.; Talapin, D. V.; Weller, H. Monitoring Surface Charge Migration in the Spectral Dynamics of Single CdSe/CdS Nanodot/Nanorod Heterostructures. *Phys. Rev. B* **2005**, *72*, 205339.
26. Verberk, R.; van Oijen, A.; Orrit, M. Simple Model for the Power-Law Blinking of Single Semiconductor Nanocrystals. *Phys. Rev. B* **2002**, *66*, 233202.
27. Gómez, D. E.; van Embden, J.; Jasieniak, J.; Smith, T. A.; Mulvaney, P. Blinking and Surface Chemistry of Single CdSe Nanocrystals. *Small* **2006**, *2*, 204–208.
28. Issac, A.; von Borczyskowski, C.; Cichos, F. Correlation between Photoluminescence Intermittency of CdSe Quantum Dots and Self-Trapped States in Dielectric Media. *Phys. Rev. B* **2005**, *71*, 161302.
29. Frantsuzov, P.; Marcus, R. Explanation of Quantum Dot Blinking without the Long-Lived Trap Hypothesis. *Phys. Rev. B* **2005**, *72*, 155321.
30. Tang, J.; Marcus, R. A. Mechanisms of Fluorescence Blinking in Semiconductor Nanocrystal Quantum Dots. *J. Chem. Phys.* **2005**, *123*, 054704.
31. Klimov, V. I.; Mikhailovsky, A.; McBranch, D.; Leatherdale, C. A.; Bawendi, M. G. Quantization of Multiparticle Auger Rates in Semiconductor Quantum Dots. *Science* **2000**, *287*, 1011–1013.
32. Sewall, S. L.; Cooney, R. R.; Anderson, K. E. H.; Dias, E. A.; Sagar, D. M.; Kambhampati, P. State-Resolved Studies of Biexcitons and Surface Trapping Dynamics in Semiconductor Quantum Dots. *J. Chem. Phys.* **2008**, *129*, 084701.
33. Jones, M.; Lo, S. S.; Scholes, G. D. Quantitative Modeling of the Role of Surface Traps in CdSe/CdS/ZnS Nanocrystal Photoluminescence Decay Dynamics. *Proc. Natl. Acad. Sci. U.S.A.* **2009**, *106*, 3011–3016.
34. Galland, C.; Ghosh, Y.; Steinbrück, A.; Sykora, M.; Hollingsworth, J. A.; Klimov, V. I.; Htoon, H. Two Types of Luminescence Blinking Revealed by Spectroelectrochemistry of Single Quantum Dots. *Nature* **2011**, *479*, 203–207.
35. Cordones, A. A.; Bixby, T. J.; Leone, S. R. Evidence for Multiple Trapping Mechanisms in Single CdSe/ZnS Quantum Dots from Fluorescence Intermittency Measurements over a Wide Range of Excitation Intensities. *J. Phys. Chem. C* **2011**, *115*, 6341–6349.

36. Kern, S. J.; Sahu, K.; Berg, M. A. Heterogeneity of the Electron-Trapping Kinetics in CdSe Nanoparticles. *Nano Lett.* **2012**, *11*, 3493–3498.
37. Malko, A. V.; Park, Y.-S.; Sampat, S.; Galland, C.; Vela, J.; Chen, Y.; Hollingsworth, J. A.; Klimov, V. I.; Htoon, H. Pump-Intensity- and Shell-Thickness-Dependent Evolution of Photoluminescence Blinking in Individual Core/Shell CdSe/CdS Nanocrystals. *Nano Lett.* **2011**, *11*, 5213–5218.
38. Durisic, N.; Godin, A. G.; Walters, D.; Grütter, P.; Wiseman, P. W.; Heyes, C. D. Probing the "Dark" Fraction of Core–Shell Quantum Dots by Ensemble and Single Particle pH-Dependent Spectroscopy. *ACS Nano* **2011**, *5*, 9062–9073.
39. Cordones, A. A.; Bixby, T. J.; Leone, S. R. Direct Measurement of Off-State Trapping Rate Fluctuations in Single Quantum Dot Fluorescence. *Nano Lett.* **2011**, *11*, 3366–3369.
40. Kambhampati, P. Hot Exciton Relaxation Dynamics in Semiconductor Quantum Dots: Radiationless Transitions on the Nanoscale. *J. Phys. Chem. C* **2011**, *115*, 22089–22109.
41. Krauss, T. D.; Peterson, J. J. Quantum Dots: A Charge for Blinking. *Nat. Mater.* **2012**, *11*, 14–16.
42. Padilha, L. A.; Robel, I.; Lee, D. C.; Nagpal, P.; Pietryga, J. M.; Klimov, V. I. Spectral Dependence of Nanocrystal Photoionization Probability: The Role of Hot-Carrier Transfer. *ACS Nano* **2011**, *5*, 5045–5055.
43. Mcguire, J. A.; Sykora, M.; Robel, I.; Padilha, L. A.; Joo, J.; Pietryga, J. M.; Klimov, V. I. Spectroscopic Signatures of Photocharging Due to Hot-Carrier Transfer in Solutions of Semiconductor Nanocrystals under Low-Intensity Ultraviolet Excitation. *ACS Nano* **2010**, *4*, 6087–6097.
44. Califano, M. Off-State Quantum Yields in the Presence of Surface Trap States in CdSe Nanocrystals: The Inadequacy of the Charging Model To Explain Blinking. *J. Phys. Chem. C* **2011**, *115*, 18051–18054.
45. Schwartz, O.; Tenne, R.; Levitt, J. M.; Deutsch, Z.; Itzhakov, S.; Oron, D. Colloidal Quantum Dots as Saturable Fluorophores. *ACS Nano* **2012**, *6*, 8778–8782.
46. Saba, M.; Minniberger, S.; Quochi, F.; Roither, J.; Marceddu, M.; Gocalinska, A.; Kovalenko, M. V.; Talapin, D. V.; Heiss, W.; Mura, A.; *et al.* Exciton–Exciton Interaction and Optical Gain in Colloidal CdSe/CdS Dot/Rod Nanocrystals. *Adv. Mater.* **2009**, *21*, 4942.
47. Klimov, V. I.; Mcguire, J. A.; Schaller, R. D.; Rupasov, V. I. Scaling of Multiexciton Lifetimes in Semiconductor Nanocrystals. *Phys. Rev. B* **2008**, *77*, 195324.
48. Tice, D. B.; Frederick, M. T.; Chang, R. P. H.; Weiss, E. A. Electron Migration Limits the Rate of Photobrightening in Thin Films of CdSe Quantum Dots in a Dry N_2(g) Atmosphere. *J. Phys. Chem. C* **2011**, *115*, 3654–3662.
49. Shepherd, D. P.; Whitcomb, K. J.; Milligan, K. K.; Goodwin, P. M.; Gelfand, M. P.; van Orden, A. Fluorescence Intermittency and Energy Transfer in Small Clusters of Semiconductor Quantum Dots. *J. Phys. Chem. C* **2010**, *114*, 14831–14837.
50. Wang, C.; Wehrenberg, B. L.; Woo, C. Y.; Guyot-Sionnest, P. Light Emission and Amplification in Charged CdSe Quantum Dots. *J. Phys. Chem. B* **2004**, *108*, 9027–9031.
51. Califano, M.; Franceschetti, A.; Zunger, A. Lifetime and Polarization of the Radiative Decay of Excitons, Biexcitons, and Trions in CdSe Nanocrystal Quantum Dots. *Phys. Rev. B* **2007**, *75*, 115401.
52. Oron, D.; Kazes, M.; Shweky, I.; Banin, U. Multiexciton Spectroscopy of Semiconductor Nanocrystals under Quasi-Continuous-Wave Optical Pumping. *Phys. Rev. B* **2006**, *74*, 115333.
53. Franceschetti, A.; Zunger, A. Optical Transitions in Charged CdSe Quantum Dots. *Phys. Rev. B* **2000**, *62*, R16287–R16290.
54. Wang, L.-W.; Califano, M.; Zunger, A.; Franceschetti, A. Pseudopotential Theory of Auger Processes in CdSe Quantum Dots. *Phys. Rev. Lett.* **2003**, *91*, 056404.
55. Ji, X.; Copenhaver, D.; Sichmeller, C.; Peng, X. Ligand Bonding and Dynamics on Colloidal Nanocrystals at Room Temperature: The Case of Alkylamines on CdSe Nanocrystals. *J. Am. Chem. Soc.* **2008**, *130*, 5726–5735.
56. Talapin, D. V.; Koeppe, R.; Gotzinger, S.; Kornowski, A.; Lupton, J. M.; Rogach, A. L.; Benson, O.; Feldmann, J.; Weller, H. Highly Emissive Colloidal CdSe/CdS Heterostructures of Mixed Dimensionality. *Nano Lett.* **2003**, *3*, 1677–1681.
57. Marceddu, M.; Saba, M.; Quochi, F.; Lai, A.; Huang, J.; Talapin, D. V.; Mura, A.; Bongiovanni, G. Charged Excitons, Auger Recombination and Optical Gain in CdSe/CdS Nanocrystals. *Nanotechnology* **2011**, *23*, 015201.